# The Design of High-$T_c$ Superconductors – Room Temperature Superconductivity?

J.L. Tallon*, J.G. Storey and B. Mallett

MacDiarmid Institute for Advanced Materials and Nanotechnology, Industrial Research Ltd., P.O. Box 31310, Lower Hutt, New Zealand.

***Abstract*** **– This year is the centennial of the discovery of superconductivity and the 25th anniversary of the discovery of high-$T_c$ super-conductors (HTS). Though we still do not fully understand how HTS work, the basic rules of design can be determined from studying their systematics. We know what to do to increase $T_c$ and, more importantly, what to do to increase critical current density $J_c$. This in turn lays down a challenge for the chemist. Can the ideal design be synthesized? More importantly, what are the limits? Can one make a room-temperature superconductor? In fact fluctuations place strict constraints on this objective and provide important guidelines for the design of the ideal superconductor.**

Preprint of plenary SCC paper submitted to *Physica C* (should be cited accordingly)
Submitted to ESNF December 14, 2011; accepted January 07, 2012. Reference No. ST294; Category 1,2.

***Keywords*** **– high-temperature superconductor, rare-earth cuprate, room-temperature superconductivity**

## I. INTRODUCTION

A quarter of a century on from the discovery of cuprate high-$T_c$ superconductors (HTS) there is still no agreed mechanism for the pairing of carriers. In principle this could be expected to prevent the rational design of better HTS. But in fact we know enough about their behavior to assemble some clear guidelines as to how to increase $T_c$ and in practical terms how to increase the critical current density, $J_c$. A much talked about goal, even here at this conference, is the grand hope of room temperature superconductivity. But is this possible? And would such materials be useful? These important issues are the focus of this paper.

HTS cuprates are indeed remarkable materials but they are complex and it is this complexity that compromises both their understanding and their optimization. At first sight they seem clearly to be non-BCS superconductors. But is this really true? There are other complicating factors that conspire to obscure the true situation. We list these and then illustrate how these various factors play out in the complex phenomenology of HTS.

* Corresponding author. e-mail: J.Tallon@irl.cri.nz. Invited paper presented at EUCAS, 19-23 September 2011.

## II. WHAT DETERMINES $T_c$?

In a conventional weak-coupling *d*-wave super-conductor one can say rather simplistically that $T_c$ is determined by the magnitude of the anisotropic *d*-wave gap, $\Delta_0$, which can be considered to be identical to the superconducting (SC) order parameter, $\Delta_0'$. The relation is:

$$2.14\, k_B\, T_c^{mf} = \Delta_0 = 2\, \hbar\omega_B \exp[-1/(N(E_F)\, V)] \qquad (1)$$

where usually one would just write $T_c$ but it is necessary to emphasize that it is in fact the mean-field (mf) $T_c$ value, $T_c^{mf}$, because fluctuations play such an important role in HTS physics. In Equation (1) $\hbar\omega_B$ is the energy scale of the pairing boson, $N(E_F)$ is the density of states (DOS) at the Fermi level and $V$ is the pairing interaction.

Some of the complications include: (i) In the underdoped region there is a pseudogap which depletes the DOS around the (π,0) antinodes. (ii) In the overdoped region the 2D electronic structure leads to a van Hove singularity (vHs) which strongly enhances the DOS, which in fact diverges at the singularity. Clearly this can have a major effect on $T_c$ through the exponential dependence on $\lambda = N(E_F)\, V$. (iii) The pairing boson is generally considered to be AF spin fluctuations or paramagnons, so that the energy scale $\hbar\omega_B$ is likely to be of the order of $J$ the magnetic superexchange interaction energy. This is an order of magnitude higher than the Debye energy so it is easy to see that in combination with the vHs it is quite possible, using Equation (1) to achieve room temperature superconductivity. It is this possibility that we wish to assess. Finally, (iv) as noted, there are strong SC fluctuations present both above and below $T_c$ which suppress $T_c$ below $T_c^{mf}$.

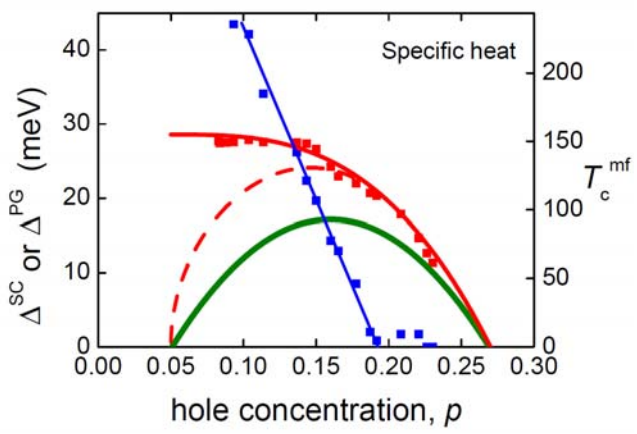


**Fig. 1.** Red data points show the SC energy gap $\Delta_0$ and blue the pseudogap energy $E_g$ from specific heat studies on $Y_{0.8}Ca_{0.2}Ba_2Cu_3O_{7-\delta}$. For a BCS *d*-wave superconductor $T_c$ is given by Eq. (1) and hence the solid red curve with right-hand scale. A $T_c$ of 150 K is expected based on the energy gap. But the pseudogap suppresses $T_c$ (dashed curve) with maximum $T_c$ now of 125 K. Moreover, SC fluctuations suppress $T_c$ even further giving $T_c^{max} \approx 90$ K.

Figure 1 summarizes these effects in the Y123 system, $Y_{0.8}Ca_{0.2}Ba_2Cu_3O_{7-\delta}$. Data points show $\Delta_0$ (red) and $E_g$ (blue) determined from specific heat studies [1]. Infrared *c*-axis ellipsometry studies confirm this data in all respects [2]. Using Equation (1) we can thus calculate the doping dependent $T_c(p)$ from $\Delta_0(p)$ – solid red curve – which reveals an expected $T_c$ for this system of 150 K if weak-coupling BCS were to apply. However, with the opening of the pseudogap at $p \approx 0.19$ holes/Cu the order parameter, $\Delta_0'$, is no longer equal to the SC gap $\Delta_0$ [3] but is suppressed below $\Delta_0$, and $T_c^{mf} = \Delta_0'/2.14k_B$ is also suppressed – dashed red curve. $T_c^{max}$ falls to about 125 K and $T_c(p)$ is now dome shaped. An idea of the suppression of $\Delta_0'$ can be derived from the model due to Bilbro and McMillan [3]. If $\Delta_0(\mathbf{k})$ and $E_g(\mathbf{k})$ have the same **k**-space symmetry around the Fermi surface then

$$(2.14\, k_B\, T_c)^2 \;=\; \Delta_0'^2 \;=\; \Delta_0^2 - E_g^2 \qquad (2)$$

Next, there is the role of strong SC fluctuations. By an entropy balance procedure the suppression of $T_c$ below $T_c^{mf}$ has been determined for $Y_{0.8}Ca_{0.2}Ba_2Cu_3O_{7-\delta}$ (Y123) and $Bi_2Sr_2CaCu_2O_{8+\delta}$ (Bi2212) [4]. The effects are of the order of only 5 to 10 K on the overdoped side but for optimal and underdoped samples the reduction in $T_c$ is of the order of 30 K for Y123 and 60 K for Bi2212. The result is summarized in Figure 1 by the solid green curve for Y123. In this way $T_c^{max}$ is finally reduced from 125 K to around 90 K. In the light of these ideas, strategies to increase $T_c$ would include reducing fluctuations (by e.g. increasing interlayer coupling or increasing external pressure) and reducing the impact of the pseudogap. Because $E_g \approx J\,(1 - p/0.19)$ [1] one approach might be to decrease $J$ by for example increasing ion size and thereby decreasing orbital overlap. In fact increasing ion size is an established strategy for increasing $T_c$ [5,6]. This is discussed in more detail in the next section.

Qualitatively, the above discussion describes the basic effects of the pseudogap and SC fluctuations in suppressing $T_c$. These issues can be addressed in rational ways. In addition one has the opportunity to control the DOS by shifting the vHs closer to the Fermi level. The location of the vHs has been shown to account for the differences in $T_c^{max}$ observed in Bi2201, Bi2212 and Tl2201 by simply assuming the same pairing interaction in each case [7]. We now examine in more quantitative detail the effects of ion size and their impact on $T_c$.

## III. ROUTES TO INCREASE $T_c$ – ION-SIZE CORRELATIONS

Twenty years ago a remarkable correlation of $T_c^{max}$ with a certain bond valence sum (BVS) parameter, $V_+$, was presented [8] that continues to represent the best correlation of $T_c$ values with any structural parameter within the class of HTS cuprates. This is reproduced in Figure 2 (solid squares) and includes 19 different cuprates. Here $V_+ = 6 - V_{Cu} - V_{O2} - V_{O3}$ where $V_{Cu}$, $V_{O2}$ and $V_{O3}$ are the planar copper and oxygen bond valence sums calculated using refined atomic coordinates from neutron diffraction. The parameter $V_+$ was introduced in an attempt to characterize the distribution of doped charge between copper and oxygen orbitals. Another parameter $V_-$ ($= 2 + V_{Cu} - V_{O2} - V_{O3}$) was introduced to estimate the total doped charge.

In addition to describing charge distribution, this $V_+$ parameter is a measure of in-plane stress with large negative values indicating compression and positive values indicating tensile extension [9]. The correlation underscores the general rule that substitution of a larger ion results in an increase in $T_c^{max}$ [5,6], as already noted.

To that early data we add additional data (crosses) for the series $LnBa_2Cu_3O_{7-\delta}$ where Ln = La, Nd, Sm, Gd, Dy and Yb [10], and for $Y(Ba_{1-x}Sr_x)_2\ Cu_3O_{7-\delta}$ [11]. This series exhibits a systematic in-plane compression as the size of the lanthanide rare earth is reduced and then Sr replaced for Ba. The correlation is conserved right across this series. The upshot of all this is that an overall strategy for increasing $T_c$ lies in substituting, wherever possible, larger ions for those in the parent compound. It would suggest e.g. that the highest $T_c$ (> 150 K) might be found in the system $HgRa_2Ca_2Cu_3O_8$ were it possible, or safe, to synthesize.

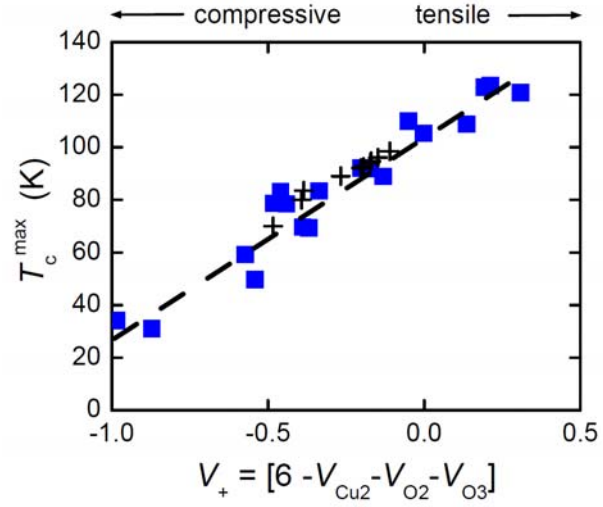


**Fig. 2.** $T_c^{max}$ plotted versus the bond-valence sum (BVS) parameter $V_+ = 6 - V_{Cu} - V_{O2} - V_{O3}$ for 19 different HTS cuprates (filled squares) and for $LnBa_2Cu_3O_{7-\delta}$ and $Y(Ba_{1-x}Sr_x)_2Cu_3O_{7-\delta}$ (crosses) which show a progressive decrease in $T_c^{max}$ as the basal plane is compressed due to reduction in ion size.

## IV. ROUTES TO INCREASE $T_c$ – APICAL OXYGEN

By way of introduction to this section we make two observations. Firstly, the top-most data points in Figure 2 are for three-layer cuprates and here one has to choose whether to calculate $V_+$ for the inner $CuO_2$ layer or the outer $CuO_2$ layer. It turns out that the correlation breaks down completely if the calculation is done for the outer layer – values are far too negative. The data shown are for the inner layer. This immediately suggests that it is the inner layer (where the apical oxygen is absent) that sets the magnitude of $T_c^{max}$.

Secondly, we consider the effects of external pressure. A profound paradox lies in the fact that, as we have just seen, *internal* pressure arising from ion-size effects decreases $T_c^{max}$ while, in sharp contrast, *external* pressure is well known to raise $T_c^{max}$ [12]. To anticipate the next section, it is quite possible that this external pressure effect is to reduce fluctuations so that $T_c$

rises towards its upper ceiling of $T_c^{mf}$, while the ion-size effect probably involves a distortion of the Fermi surface so that the vHs moves closer to $E_F$.

But here we focus on a different effect arising from external pressure. In the case of optimally-doped $Bi_2Sr_2Ca_2Cu_3O_{10+\delta}$ $T_c$ was found to rise with increasing pressure from 110 K to a maximum at ≈ 125 K then falls before rising again towards 140 K [13]. The reason is that the inner $CuO_2$ layer is underdoped relative to the two outer $CuO_2$ layers in this three-layer cuprate. Application of pressure causes charge transfer from the $Bi_2O_2$ layer so that first the outer layers optimize (leading to a peak at $T_c \approx 125$ K) and then at higher pressure the otherwise less-doped inner layer optimizes with $T_c > 140$ K. Thus again the higher $T_c$ value seems to be associated with the inner layer with its missing apical oxygen. The conclusion would seem to be that it is preferable to remove, or at least displace away, the apical oxygen.

A further conclusion is that if we could arrange for a more even distribution of charge in three-layer cuprates then we might access these much larger $T_c$ values seen under pressure. One straightforward way to achieve a more even charge distribution (and hence higher $T_c$) is to displace the apical oxygen away from the outer $CuO_2$ layers. This is precisely what happens as one progresses from $Bi_2Sr_2Ca_2Cu_3O_{10+\delta}$ to $Tl_2Ba_2Ca_2Cu_3O_{10+\delta}$ to $HgBa_2Ca_2Cu_3O_{8+\delta}$. Figure 3 shows $T_c^{max}$ plotted versus the Cu2-O4 apical bond-length and it shows a direct correlation, as expected. It remains to be seen whether in fact the charge distribution between the inner and outer layers becomes progressively more uniform with Bi → Tl → Hg but it is certainly the case that $T_c$ versus $P$ exhibits a single hump in the case of $HgBa_2Ca_2Cu_3O_{8+\delta}$ [14], suggesting that the charge distribution is much more uniform for this system.

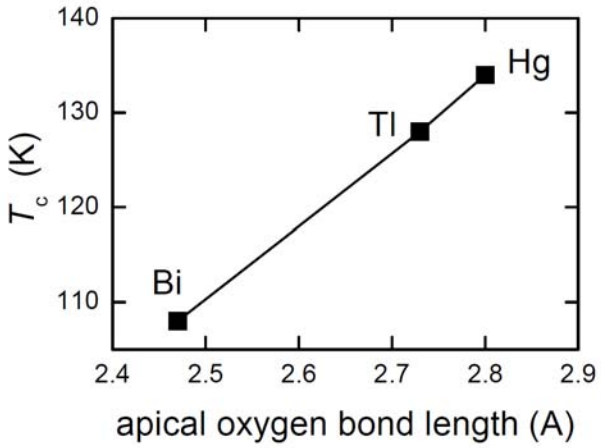


**Fig. 3.** $T_c^{max}$ plotted versus the apical oxygen bond length for $Bi_2Sr_2Ca_2Cu_3O_{10+\delta}$, $Tl_2Ba_2Ca_2Cu_3O_{10+\delta}$ and $HgBa_2Ca_2Cu_3O_{8+\delta}$. As the apical bond length increases the charge distribution between the inner and outer $CuO_2$ layers becomes more uniform.

## V. SUPERCONDUCTING FLUCTUATIONS AND MEAN-FIELD $T_c$

We now analyze in detail the effect of SC fluctuations from the electronic specific heat. Using a high-resolution differential technique the electronic specific heat can be separated from the

much larger phonon term [1,4]. In the following we drop the descriptor 'electronic' for the specific heat, entropy, etc. The specific heat coefficient $\gamma(T) \equiv C_P/T$ is shown in Figure 4(a) for Y123 close to critical doping $p_{crit} \approx 0.19$ where the pseudogap is absent and the vHs is sufficiently remote that $\gamma_n(T)$ is constant (dashed line). Because the integrated area under $\gamma(T)$ is entropy, $S(T)$, then by entropy conservation the grey shaded area must equal the hatched area between $T_c$ and $T_c^{mf}$ which thus enables $T_c^{mf}$ , $\gamma_s^{mf}(T)$ and $\Delta\gamma^{mf}$ to be determined. The dashed magenta curve is the theoretical BCS mean field $\gamma(T)$ and shows that once fluctuations are corrected for the behavior is conventional BCS.

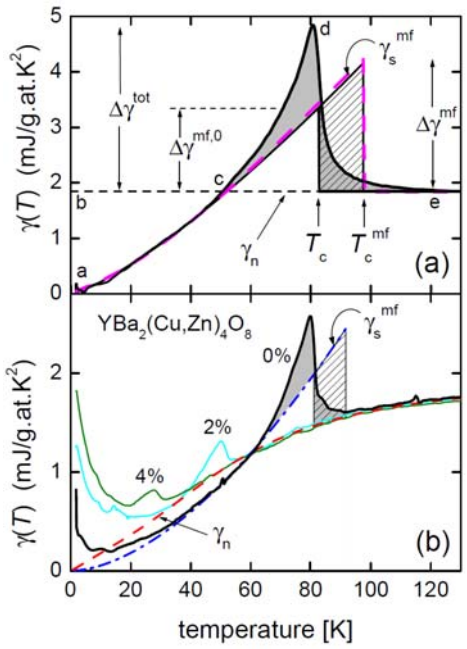


**Fig. 4.** Plots of the electronic specific heat coefficient $\gamma(T)$ for (a) Y123 with $p \approx 0.19$ and (b) Y124 showing the analysis of SC fluctuations. By entropy conservation the area *abc* equals the area *cde*. The grey shaded area is the fluctuation entropy which also by entropy conservation must equal the hatched area between $T_c$ and $T_c^{mf}$. In this way $T_c^{mf}$ and the mf jump in $\gamma$, $\Delta\gamma^{mf}$, can be determined. The dashed magenta curve is the theoretical *d*-wave BCS mf $\gamma(T)$, $\gamma_s^{mf}(T)$. In (a) the normal-state $\gamma$, $\gamma_n(T)$, is constant (dashed line); while in (b) where Y124 is underdoped the pseudogap suppresses $\gamma_n(T)$ (red dashed curve) according to Eq. (3). Inclusion of 2% and 4% Zn suppresses $T_c$ and shows that Eq. (3) is accurate.

We have carried out this analysis for many dopings across the phase diagram and also for Bi2212 where the full ARPES-derived dispersion was used including the vHs (which is closer to $E_F$ than is the case for Y123). For under-doped samples where the pseudogap is present $\gamma_n(T)$ is suppressed as $T \rightarrow 0$ so we use a triangular gap model [4]:

$$\gamma_n(T) = \gamma_0 \times \{1 - \varepsilon^{-1} \tanh(\varepsilon) \times \ln[\cosh(\varepsilon)]\} \qquad (3)$$

where $\varepsilon = E_g/2k_BT$. This is illustrated in Figure 4(b) which shows $\gamma(T)$ for $YBa_2Cu_4O_8$ (Y124). The dashed red curve is Equation (3). Data is also shown for 2% Zn (cyan curve) and 4% Zn

(green curve) where $T_c$ is strongly suppressed. Above $T_c$ these curves nicely coincide with the red dashed curve thus confirming our model, Equation (3). Notably, the size of $\Delta\gamma^{mf}$ is much diminished relative to that in Figure 4(a) and this shows the effect of the pseudogap in weakening the SC state.

The resultant doping-dependent $T_c^{mf}$ and $\Delta\gamma^{mf}$ values for Y123 and Bi2212 are reported elsewhere [4]. We reproduce the $T_c^{mf}(p)$ and $T_c(p)$ data for Bi2212 in Figure 5 plotted in the *T*-*p* plane (circles and error bars). While $T_c^{max} \approx 90$ K we find $T_c^{mf}$ reaches as high as 150 K. That is, $T_c$ is reduced by as much as 60 K due to strong SC fluctuations. On the overdoped side fluctuations are weaker and $T_c$ is reduced by only 15 to 20 K. As noted, if one could suppress SC fluctuations then it would be possible to achieve these very high $T_c$ values in the Bi2212 system. Incidentally, if pressure were to diminish fluctuations by e.g. exhancing the interlayer coupling then this might account for the unusual pressure effect on $T_c^{max}$ where the coefficient is positive and very large (4.5 K/GPa).

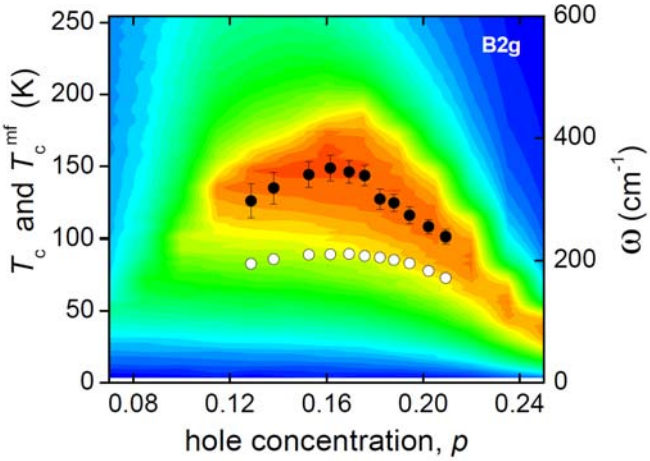


**Fig. 5.** $T_c$ (open circles) and $T_c^{mf}$ (filled circles) determined from fluctuation analysis for $Bi_2Sr_2CaCu_2O_{8+\delta}$ plotted versus doping, *p*. The background shows a false color plot of $B_{2g}$ Raman scattering for $HgBa_2CuO_{4+\delta}$ calculated from the ARPES derived dispersion and fitted to the observed $B_{2g}$ scattering for Hg1201. The intensity ridge traces out the SC order parameter $\Delta_0'$. The scales are such that $\Delta_0' = 2.4\ k_B\ T_c^{mf}$ across the entire range.

Our aim in Figure 5 is not only to present values of $T_c^{mf}$ but to compare $\Delta_0$ and $T_c^{mf}$ and, in the light of Equation (1), to test the BCS ratio. In the background is a false color plot of $B_{2g}$ Raman scattering intensity for $HgBa_2CuO_{4+\delta}$ (Hg1201) calculated from the ARPES derived dispersion and fitted to the observed $B_{2g}$ Raman intensity for Hg1201 [15] by adjusting $\Delta_0(p)$ and $E_g(p)$. The intensity ridge shows the contour of the SC order parameter $\Delta_0'(p)$. The left- and right-hand scales are such that $\Delta_0' = 2.4\ k_B\ T_c^{mf}$ across the entire range. That is, a nearly weak-coupling BCS ratio is preserved across the entire phase diagram, even in the presence of the pseudogap. This clearly is not satisfied if the BCS ratio is constructed from the observed $T_c$ (open circles) rather than $T_c^{mf}$, where $2\Delta_0'/k_B\ T_c$ then reaches as high as 8. This typically large

magnitude of $2\Delta_0'/k_B\ T_c$ has been a long-standing puzzle and a key, though erroneous, argument for non-BCS behavior.

If we use the values of $\Delta_0$ obtained from specific heat (see Figure 1) then we obtain $\Delta_0 = 2.5k_BT_c^{mf}$ across the overdoped region for both Y,Ca123 and Bi2212 [4]. (Of course as $p$ falls below 0.19, and the pseudogap opens, $\Delta_0'$ starts to fall below $\Delta_0$ so we cannot extend this test across the underdoped region). Alternatively, if we use the values of $\Delta_0$ for Y,Ca123 obtained from infrared spectroscopy [2] then we obtain $\Delta_0 = 2.2\ k_B\ T_c^{mf}$ across the overdoped region [4] in excellent agreement with the weak-coupling BCS ratio. We conclude from all this that the behavior is nearly weak-coupling BCS from the perspective of both the universal jump $\Delta\gamma^{mf}$, and the ratio $2\Delta_0'/k_BT_c^{mf}$.

## VI. ROOM TEMPERATURE SUPERCONDUCTIVITY?

We now examine the implications of these results for the prospects of room-temperature SC. We have noted that in principle the BCS formula can enable $T_c \approx 300$ K, but actually this is the mean-field value, $T_c^{mf}$, and we have to ask how much $T_c$ will be diminished below $T_c^{mf}$ due to SC fluctuations. Already in the case of Bi2212 one must have $T_c^{mf} \approx 150$ K in order to achieve $T_c \approx 90$ K.

The electronic specific heat in the neighborhood of $T_c$ has a mf term and a fluctuation term: $C_P = C^{mf} + C^{fluc}$, where the latter term for an isotropic superconductor scales as $\xi_0^{-3}$, where $\xi_0$ is the coherence length at $T = 0$. For aluminum with $T_c = 1.2$ K it is found that $\xi_0 = 1.6$ μm [16] whereas for HTS with typically $T_c = 90$ K $\xi_0 = 1.6$ nm. Accordingly fluctuations are a billion times stronger in the cuprates than in aluminum.

Now $T_c$ is reduced according to $T_c = T_c^{mf} - \Delta T_c$, and the cross-hatched area in Figure 4 is of the order of $\Delta T_c \times \gamma_n$. This has to equal the fluctuation entropy $\int \gamma^{fluc}(T)\ dT$. For an anisotropic quasi-two-dimensional SC the magnitude of the fluctuation specific heat scales as $\xi_0^{-2}\times d_b^{-1}$ where $d_b$ is the block layer spacing between $CuO_2$ bilayers. Thus,

$$\Delta T_c \times \gamma_n \propto\ \xi_0^{-2} \propto\ \Delta_0^{\,2} \propto\ (T_c^{mf})^2 \qquad (4)$$

and therefore

$$T_c = T_c^{mf}\,(1 - T_c^{mf}/T_0) \qquad (5)$$

so that $T_c$ is diminished quadratically by the magnitude of $T_c^{mf}$. It is straightforward from the former fluctuation analysis to determine $T_0$ for each of the systems we have investigated, $Bi_2Sr_2CaCu_2O_{8+\delta}$, $Y_{0.8}Ca_{0.2}Ba_2Cu_3O_{7-\delta}$ and $YBa_2Cu_3O_{7-\delta}$. We therefore plot in Figure 6 values of $T_c$ as a function of $T_c^{mf}$ for each of these systems. The asterices correspond to the observed optimum doping in the three systems. What is found is that as $T_c^{mf}$ rises (due e.g. to shifting the vHs to lower doping, or increasing the pairing interaction) $T_c$ passes through a maximum and then falls with further increase in $T_c^{mf}$. $YBa_2Cu_3O_{7-\delta}$, which has the strongest interlayer coupling admits the highest $T_c \approx 160$ K when $T_c^{mf} \approx 300$ K, but $Y_{0.8}Ca_{0.2}Ba_2Cu_3O_{7-\delta}$ with its

partially disordered chains has weaker interlayer coupling and $T_c$ barely rises above 100 K and has fallen to 80 K when $T_c^{mf} \approx 300$ K. The situation is worse still for $Bi_2Sr_2CaCu_2O_{8+\delta}$, for which the maximal $T_c$ does not appear to exceed 96 K. This illustrates that in these HTS materials there is little prospect of achieving coherent superconductivity near room temperature.

The reason is clear enough. If the coherence length, $\xi_{ab}$, is 1.6 nm for a $T_c^{mf} \approx 100$ K superconductor then $\xi_{ab} \approx 0.5$ nm for $T_c^{mf} \approx 300$ K. This is less than the in-plane unit cell parameter and under such circumstances adjacent orbitals will not overlap coherently. Moreover, because:

$$\xi_{ab} = \hbar v_F/\pi\Delta_0 = \hbar v_F\,(2.14\pi\, T_c^{mf})^{-1} \qquad (6)$$

where $v_F$ is the Fermi velocity, then the only route to avoid this problem would be to find a system with a substantially larger Fermi velocity and hence a larger carrier concentration. As $v_F \propto \sqrt{n}$ this would require at the very least a quadrupling of the carrier density. This is not achievable in the HTS cuprates and therefore requires a fundamentally different HTS system to achieve a room temperature coherent SC state and at such carrier densities magnetic interactions are likely to be rather weak.

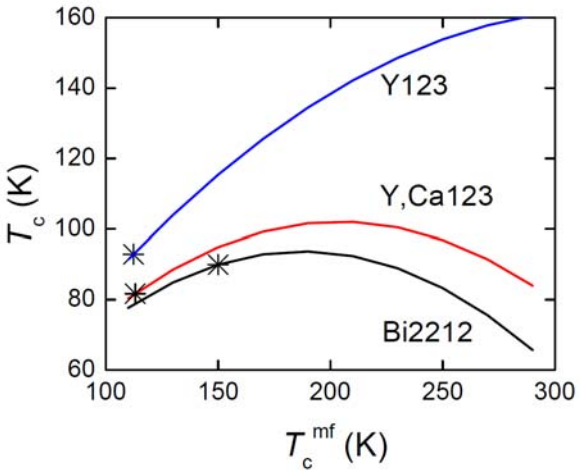


**Fig. 6.** $T_c$ plotted versus $T_c^{mf}$ for $Bi_2Sr_2CaCu_2O_{8+\delta}$, $Y_{0.8}Ca_{0.2}Ba_2Cu_3O_{7-\delta}$ and $YBa_2Cu_3O_{7-\delta}$ using Eq. (5) with $T_0$ determined from the analysis illustrated in Figure 4. This shows that as $T_c^{mf}$ is progressively increased so the depression in $T_c$ due to SC fluctuations increases, to the extent that $T_c$ eventually falls as $T_c^{mf}$ continues to rise. The asterices show the location of $T_c^{max}$ as observed at optimal doping.

In summary, we have shown that there are a number of systematic strategies to increase $T_c^{max}$ at optimum doping in the cuprates. These include (i) expansion of the lattice by substitution of larger ions, and (ii) displacement (or total removal) of the apical oxygen away from the outer $CuO_2$ layers in a two- or three-stack cuprate. It is also crucial to (iii) shift the van Hove singularity as much as possible to low doping i.e. closer to the Fermi level to gain the benefit of the large DOS where the pairing interaction is stronger at low doping. The ideal cuprate therefore (iv) is probably the so-called infinite-layer system comprising alternating $CuO_2$ layers and Sr or Ca layers. If it were possible to substitute Ba for Sr in the infinite layer system then greater

$T_c^{max}$ values could be anticipated. Moreover the infinite-layer system possesses very strong interlayer coupling so can be expected to potentially exhibit higher critical currents. It would have to be doped to $p \approx 0.19$ holes per Cu by alkali substitution for Ca, Sr or Ba.

Analysis of electronic specific heat data shows that (v) the universal BCS ratios are satisfied across the phase diagram and (vi) $T_c$ is shifted down rather substantially from $T_c^{mf}$ – as much as 60 K in the case of $Bi_2Sr_2CaCu_2O_{8+\delta}$. This is due to the presence of strong superconducting fluctuations high above $T_c$. This means that (vii) room temperature superconductivity is probably unachievable. With $T_c^{mf}$ as high as 300 K the actual $T_c$ would be shifted down to around 160 K – already the maximum observed $T_c$ in the cuprates. These effects could be mitigated if (viii) high-$T_c$ materials could be found with higher carrier concentration enabling larger coherence lengths and therefore a weaker fluctuation specific heat. As it is (ix) the cuprates display exceptional properties and efforts would probably be better placed in seeking to further develop technologies around $LnBa_2Cu_3O_7$ by increasing critical currents and developing more reliable technologies for coated conductors. That said, and in view of the above, efforts in developing novel doped versions of the infinite-layer system could be most productive.

## VIII. REFERENCES

[1] J.W. Loram *et al.*, *J. Phys. Chem. Sol.* **62** (2001) 59.
[2] L. Yu *et al.*, *Phys. Rev. Lett.* **100** (2008) 177004.
[3] G. Bilbro, W. McMillan, *Phys. Rev. B* **14** (1976) 1887.
[4] J.L. Tallon, J.G. Storey and J.W. Loram, *Phys. Rev. B* **83** (2011) 092502.
[5] G.V.M. Williams, J.L. Tallon, *Physica C* **258** (1991) 41.
[6] M. Marezio *et al.*, *Physica C* **341** (2000) 375.
[7] J.G. Storey, J.L. Tallon and G.V.M. Williams, *Phys. Rev. B* **76** (2007) 174522.
[8] J.L. Tallon, *Physica C* **168** (1990) 85.
[9] A. Mawdsley, J.L. Tallon and M.R. Presland, *Physica C* **190** (1992) 437.
[10] M. Guillaume *et al.*, *J. Phys. Cond. Mat.* **6** (1994) 7963.
[11] F. Licci *et al.*, *Phys. Rev. B* **58** (1998) 15208.
[12] N. Suresh *et al*., *Phys. Rev. B* **78** (2008) 100503(R).
[13] X.-J. Chen *et al.*, *Nature* **466** (2010) 950.
[14] L. Gao *et al.*, *Phys. Rev. B* **50** (1994) 4260.
[15] J.L. Tallon and J.G. Storey, cond-mat/0908.4430v1.
[16] H. Lohneysen *et al.*, *Physica C* **460–462** (2007) 322.